Size-dependent diffusion of 3D nanovoids in a bcc solid

Stefano Curiotto, Pierre Müller, Fabien Cheynis, Loic Corso, Elodie Bernard, Frédéric Leroy

Size-dependent diffusion of 3D nanovoids in a bcc solid

Stefano Curiotto,[1] Pierre Müller,[1] Fabien Cheynis,[1] Loic Corso,[2,1] Elodie Bernard,[2] and Frédéric Leroy[1]
[1)]*Aix Marseille Univ, CNRS, CINAM, Marseille, France*
[2)]*CEA, IRFM, F-13108 Saint Paul-lez-Durance, France*

(*Author to whom correspondence should be addressed: Stefano Curiotto: stefano.curiotto@cnrs.fr)

We have studied the diffusion of 3D nanovoids in a bcc solid by kinetic Monte Carlo simulations. The diffusion coefficient as a function of the void size increases, reaches a maximum and then decreases. The first increase is particularly interesting, as the diffusion of clusters is generally considered a decreasing function of the cluster size. We attribute this behavior to a curvature-dependent energy barrier for mass transport. We propose an analytical modeling of the void diffusion coefficient that reproduces the simulation data over the whole size range. In addition, for low temperatures and small sizes, the void diffusion coefficient versus size displays valleys, i.e. regions where the diffusion coefficient is smaller than the general trend. This behavior cannot be explained with analytical developments, and is due to the formation of compact shapes for certain magic void sizes. In these shapes the atoms at the void surface are strongly bound, displace less and thus also void diffusion is slower.

Voids play a critical role in determining mechanical, thermal, electrical and optical materials properties. Understanding the formation of voids during sintering of ceramics allows predicting the strength and the reliability of the material[1]. In metals, voids formed in the manufacturing process, can grow and merge under tensile or shear stress, leading to fracture and material failure[2]. Voids can lead to solid state dewetting of thin films[3]. Under an electric field, voids drift and coalesce, inducing failure of the electronic tracks used in circuits[4,5]. The formation of bubbles in irradiated materials is also of particular concern. They are formed by the bombardment of neutrons, heavy and light ions, electrons and γ-rays[6]. The gas contained in the bubbles can permeate out of the material, leaving voids, as found by Griffioen et al.[7]. Components of fission and fusion reactors can be significantly damaged by the formation of bubbles and voids in nuclear power plants[8]. The displacement by diffusion of voids in a material can lead to the growth of pores and understanding it is important to predict and/or avoid possible changes of the material properties. Furthermore, the diffusion of liquid inclusions in a solid matrix shows strong similarities with void diffusion[9,10] . From an analytical, continuum, point of view, the foundations of the diffusional motion of pores in solids have been established by Nichols[11], and Willertz and Shewmon[12]. The growth by coalescence and Ostwald ripening of voids has been investigated by Goodhew and coworkers (see as an example[13]) and Evans[14]. However, nanosized voids could behave differently from the predictions of continuum theories.

In this work we investigate the diffusive motion of voids of small size. While experimentally it is difficult to investigate the displacement of nanovoids in bulk materials, atomistic simulations are perfectly suited to this aim.

We use a 3D kinetic Monte Carlo (KMC) model with atoms occupying positions of a bcc lattice. This structure has been chosen because void and bubble diffusion has been historically studied for its importance in nuclear materials[11], in particular tungsten, used in fusion reactors like ITER[15], and iron (ferritic steels are candidate for both fission and fusion reactors[16]). We expect that our results will also be relevant for other structures, but the details of the void diffusion will be different. A general introduction on the KMC method can be found in[17]. In our model, each atom can jump to unoccupied nearest-neighbor sites with rates proportional to $\nu_0 \exp[-(nJ + sJ')/(kT)]$, where n is the number of nearest neighbors of the atom, J is the binding energy between nearest neighbors, s is the number of second (or next-nearest) neighbors of the atom, J' is the binding energy of second neighbors, k is the Boltzmann constant and T is the temperature. ν_0 is a jump attempt frequency that defines our time unit, we take it equal to 1 for all atoms[18]. Our simple energetic description, based on an additive binding energy, is the one used in early crystal growth studies. It allows for predicting the equilibrium shapes of crystals, calculating surface and interfacial energies, determining adsorption isotherms, and has been used for atomic modeling of epitaxy (see[21–23]). This approach is still employed by many authors, especially in KMC simulations, to predict trends, mechanisms and general behaviors (see for instance[24–27]). In a bcc lattice each position has maximum 8 nearest neighbors n and 6 second neighbors s. Within our model, atoms cannot move out of lattice positions nor to a position without neighbors. The simulation box has periodic boundary conditions, meaning that an atom going out from one side re-appears on the opposite side. We have taken J' as the energy unit (equal to 1). $\frac{J}{J'} = 1.155$ has been chosen so that the shape of a void calculated with our model, shown in figure 1, is constituted by $\{100\}$ and $\{110\}$ facets, and repro-

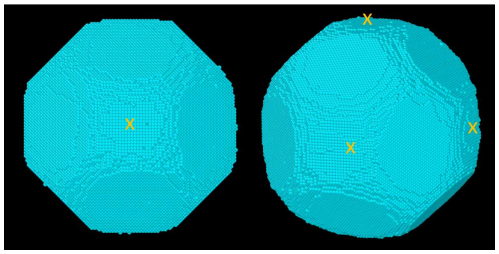

FIG. 1. Two different views of the shape of a void in a bcc lattice simulated with our KMC model. The void is a truncated dodecahedron, with $\{100\}$ and $\{110\}$ facets. The $\{100\}$ facets are marked with a yellow cross. The void radius is $36a$, $kT = 0.4J'$.

duces well the experimental shape of bubbles in tungsten[19]. It has been experimentally found that other bcc solids, like for instance Fe nanoparticles[20], display a similar equilibrium shape.

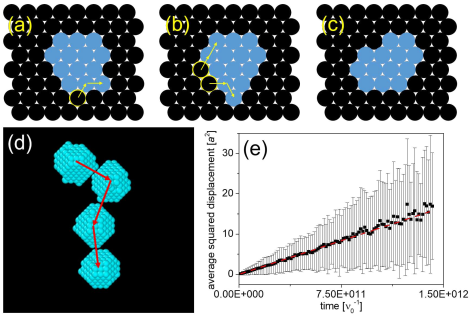

FIG. 2. (a)-(c): schematics showing the displacement of a void as a consequence of atomic displacement. Atoms at the void surface (black), move in empty positions (blue). As a result, the void center of mass displaces. (d): displacement of a void constituted by 330 empty positions, $kT = 0.5J$. (e): average squared displacement as a function of time for the void shown in (d). The error bar is the standard deviation of $< r^2 >$. Notice that when the time increases, $< r^2 >$ is based on less measurements, and thus the error increases. The slope of the linear fit through the black squares gives $< r^2 > /t$.

In the simulations, atoms at the void surface randomly diffuse, according to the jump probabilities defined above, and as a consequence of many atomic jumps voids also displace. Figures 2(a)-(c) schematically show in 2D the motion of atoms at a void surface, leading to the displacement of the void center of mass. In 3D the diffusion coefficient of a single vacancy can be written as equal to $D = \frac{1}{6}\Gamma\lambda^2$, with Γ the jump frequency and λ the jump length (see for instance[28] or the supplementary material in[29]). Within our model $\Gamma = \nu_0 \exp(\frac{-E_{vac}}{kT})$, where E_{vac} is the vacancy jump energy (jump energy of a bulk atom close to a single vacancy, i.e. $E_{vac} = 7J + 6J'$), and $\lambda = a\sqrt{3}/2$. The average square displacement $< r^2 >$ is $< r^2 >= \Gamma\lambda^2 t$. In our model D is exactly defined for a single vacancy, for which Γ and λ^2 are known; for a void D can be obtained by measuring in simulations $< r^2 > /t$, $D = \frac{1}{6}\frac{<r^2>}{t}$. Figure 2(d) shows as an example the simulation of the displacement of a void made of 330 empty positions. The void squared displacement can be measured as a function of time in the simulations using the method detailed by Bogicevic et al.[30]. The black squares in figure 2(e) show the $< r^2 >$ as a function of time for a void with 330 empty positions. The squared displacement is averaged over at least 30 measurements for each time. The slope of the linear fit through the data points shown by the red dashed line gives $< r^2 > /t$.

We have repeated the procedure for voids of different sizes and at different temperatures. Vacancies can detach from the surface of moving voids, particularly for small voids and at high temperatures, therefore small voids can change size during the diffusive motion. Thus, for small voids, the diffusion coefficient is not defined. Figure 3(a) shows the void diffusion coefficient as a function of the void size (expressed as the number of empty positions in the void N) in logarithmic scale, for different temperatures. At low temperatures, the diffusion coefficient D as a function of the cluster size does not display a monotonic curve. Valleys (discussed later) are observed for specific values of N, two of them are highlighted in figure 3b and 3c. Furthermore, considering the general trend, D increases up to a maximum from which it decreases. An isolated vacancy is slower than intermediate-size voids, and only large clusters diffuse slower than a vacancy. However the size of voids diffusing slower than vacancies decreases when the temperature increases. From analytical considerations[11], voids are expected to diffuse less when their size increases (see the supplementary material for a short summary). Interestingly, the diffusion of adsorbates in confined spaces like zeolite pores also follows a trend similar to that observed by us (D increases, reaches a maximum and then decreases)[31–33]. In that case, the maximum is reached when the adsorbate dimensions match closely those of the pores. Also other authors have found that confined spaces promote the transport of adsorbates, for instance in the case of molecules in nano-

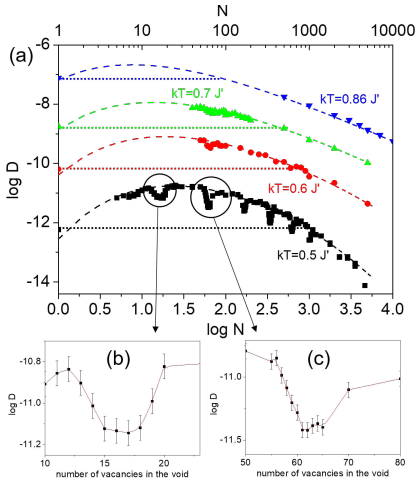

FIG. 3. (a): diffusion coefficient as a function of void size (number of empty positions N) in logarithmic scale, for different kT. Also the diffusion coefficient of single vacancies is shown. The horizontal dotted lines are useful to compare the diffusion coefficient of single vacancies with that of voids. The dashed lines show the agreement between the data points and the analytical expression of equation 1. The parameters are $\alpha = 0.3 \pm 0.2$, $E_0 = 7.7 \pm 0.1$, $E_1 = 6.76 \pm 0.09$, common for the four temperatures, and $\gamma g = 0.126 \pm 0.005, 0.059 \pm 0.005, 0.023 \pm 0.005$ and 0 for kT increasing from 0.5 J' to 0.86 J'. Some valleys are visible for kT=0.5 J', and two of them are highlighted in (b) and (c), where the void size is in linear scale. The full line is a guide for the eye.

channels[34], and for interstitial atoms of different sizes in a bcc lattice[35]. These results pertain to the diffusion of adsorbates within a network of pores, while in our study we investigate a distinct phenomenon, i.e. the diffusion of isolated voids that are not interconnected.

However, a behavior similar to that described in figure 3 has been observed and explained in 2D, for monoatomic-deep holes on surfaces[29]. The increase in mobility when N increases observed for small void sizes is due to an increase of the total jump frequency Γ related to the void curvature ($-1/R$ with R the void radius) and not only to the surface increase: larger voids are less and less concave, the atoms at the void surface are thus less bound and consequently the large-void jump rate is higher than for small voids. The rate of curvature change ($\frac{d(-1/R)}{dR} = \frac{1}{R^2} \propto N^{-2/3}$) decreases for larger voids. Therefore from a certain size it becomes negligible, and D decreases when N increases as predicted by usual analytical considerations. After these qualitative arguments, we now include the curvature effect in an expression to describe the general trends observed in figure 3a. The diffusion coefficient of a void can be written as $D \propto \Gamma\lambda^2$, in analogy with that of a single vacancy. The void jump frequency Γ is proportional to: (i) the number of atoms at the void surface ($\Gamma_{(i)} \propto R^2$); (ii) the rate of displacement of atoms at the void surface; (iii) a term to take into account the nucleation of a new facet at the void surface (only the nucleation of a new facet leads to a net displacement of the void). The displacement of atoms (term (ii)) depends on the void curvature, as written above, and we thus write $\Gamma_{(ii)} \propto \exp\frac{-(E_0+E_1/R)}{kT}$. E_0 includes both an average energy of surface diffusion and an energy for the detachment of atoms from flat surfaces. E_1/R corrects E_0 to take into account the curvature effect (for small voids the energy to displace an atom is on average larger than for large voids). Term (iii) can be written as $\Gamma_{(iii)} \propto \exp\frac{-\gamma \cdot g \cdot R}{kT}$, where γ is the step energy of the new facet and $g \cdot R$ accounts for the facet dimension (proportional to the void radius)[12,36,37]. The displacement length λ is inversely proportional to the void volume, i.e. $\lambda \propto R^{-3}$. Putting all together and considering that $R \propto N^{1/3}$:

$$D = \alpha \cdot N^{-4/3} \cdot \exp\left(-\frac{E_1 + E_0 \cdot N^{1/3} + \gamma g \cdot N^{2/3}}{kT \cdot N^{1/3}}\right) \quad (1)$$

where α includes all the proportionality factors. We have fitted the four diffusion coefficient versus size curves (dashed lines in figure 3a) with equation 1, the agreement is very good. In the fitting procedure we have used a single set of parameters α, E_1, E_0, as they do not depend on the temperature. We have considered different values of γg for the four data sets and found that γg decreases when the temperature increases from kT=0.5 J' to 0.6 and 0.7 J', and vanishes for kT=0.86 J'. This is in agreement with the known behavior of the step energy, that decreases with the temperature and vanishes above the roughening transition temperature[38,39]. Notice that for negligible γ (condition verified at high temperature) and large N, the equation correctly predicts $D \propto N^{-4/3}$, i.e. the regime of void motion limited by surface diffusion[11]. This regime is obtained for large voids at $kT = 0.7J'$ and $0.86J'$, as in figure 3(a) the slope of the $\log D$ versus $\log N$ curve reaches an asymptotic value.

Because of the γg dependence on temperature, it is not appropriate to define a diffusion energy for the voids. However, for the sake of comparison with a different phenomenon, i.e. adsorbate diffusion in porous matrices[33,35], we have measured an effective energy for the diffusion of four voids with different size. For each void size, this effective energy is found, using the common expression $D = D_0 \exp\frac{-E_{eff}}{kT}$, from the slope of the linear fit of $\ln D$ versus $1/(kT)$. As detailed in the supplementary material, we find $E_{eff} = 11.4 \pm 0.2, 10.8 \pm 0.1, 11.1 \pm 0.2$ and 11.3 ± 0.3 for N =10, 40, 90 and 310 respectively. As expected, and as also found in matrices made by a network of pores, the effective diffusion energy shows a minimum for the fastest-diffusing cluster size N=40.

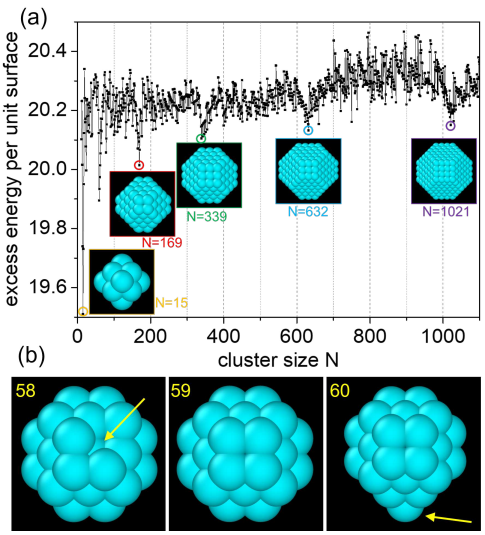

FIG. 4. (a): Excess energy per unit surface as a function of cluster size for the most cohesive shape at each N. (b): compact shapes of clusters with N=58, 59 and 60 empty positions. The most compact shape is obtained for N=59. Arrows show the missing and the additional empty positions that do not allow the clusters with N=58 and N=60 to have a compact shape.

The valleys obtained for kT=0.5 J' and still visible at kT=0.6 J' cannot be explained by general considerations on Γ or λ. Clusters with specific sizes displace slower than voids with similar dimensions because their number of empty positions is such that they can assume compact shapes, where the cohesion energy of the atoms at the void surface is maximized. Voids stay longer time in the compact shape and thus diffuse slower. Notice that the formula reported in the literature to obtain the perfect sizes of bcc dodecahedra[40,41] does not apply to bcc truncated dodecahedra. For voids of different size, we have calculated the cohesion energy of the atoms around each void for the shape that maximizes cohesion. The most cohesive shape is found in simulations by changing the shape of a

void, and taking the shape that maximizes the system cohesive energy (i.e. the sum of the binding energies of all the atoms). The excess energy is found by substrating this energy from the cohesive energy of a system without the void. The excess energy is divided by $N^{2/3}$ to obtain a value per unit surface. Figure 4a shows the excess energy of a system with a void as a function of the void size. For N=15, 59, 169, 339, 1021, minima are clearly observed. These voids can have the perfect compact shape of a symmetric truncated dodecahedron. Figure 4b shows as an example the compact shapes for voids with N=58, 59 and 60 empty positions. For N=59, the cluster has the perfect, or magic, shape of a truncated dodecahedron, with 12 $\{110\}$ and 6 $\{100\}$ complete facets, while the voids with N=58 and N=60 have either a missing or an additional empty position (see the arrows in figure 4b).

Other minima are also observed, for instance at $N = 632$. These voids can present a compact shape (see figure 4a), that is not perfectly symmetric. The minima in figure 3a correspond to the minima of figure 4a. Notice that also voids with a size close to that of perfect clusters can diffuse slowly, because the displacement of a void involves the motion of more than one atom for the nucleation of new facets. Lai et al. have explained this mechanism for 2D islands[42–44]. As an example, in a void with one vacancy more than the size showing a perfect shape, the excess vacancy can move longtime at the void surface without a clear displacement of the entire cluster, unless one or more other vacancies detach from a strongly bound position of the perfect shape, and a new void facet is formed.

The exact sizes of perfect clusters depend on the equilibrium shapes defined by our model, i.e. depend on the J/J' ratio that we have used. For larger J/J' the equilibrium shape of the voids is a less-truncated dodecahedron, and the number of vacancies of perfect size clusters is shifted towards higher values. For very large J/J', i.e. when the second-neighbors bonds can be neglected, the sizes of perfect clusters are those corresponding to not-truncated dodecahedra, i.e. N=15, 65, 175, 369, 671, 1105[40].

To summarize, we have investigated the diffusion behaviors of small 3D voids in a bcc solid. The void diffusion coefficient increases with the void size, reaches a maximum and then decreases. This trend can be explained by the curvature change when the void size increases. We have developed an analytical expression of the void diffusion coefficient that includes the curvature effect and that reproduces very well the simulation data. At low temperatures and small void sizes, the diffusion coefficient as a function of size displays valleys for voids with specific dimensions. This size effect is due to the presence of voids that can assume compact shapes where atoms are strongly bound, and therefore their displacement is more difficult.

SUPPLEMENTARY MATERIAL

The supplementary material discusses the conventionally-accepted analytical dependence of the diffusion coefficient on the cluster size in three limiting cases: when the diffusion process is limited by surface diffusion, by attachment/detachment of atoms at the void surface, and by volume diffusion. Furthermore, we also show the data points and the linear fits used to obtain the effective energies of four void sizes.

ACKNOWLEDGMENTS

This work has been supported by the ANR grant Thermotweez (ANR-22-CE09-0009-01). We thank G. Aissani for performing some of the KMC simulations.

DATA AVAILABILITY

The data that support the findings of this study are available from the corresponding author upon reasonable request.

REFERENCES

[1] F. Wakai, G. Okuma, and N. Nishiyama, Materials today - proceedings **16**, 4 (2019).
[2] W. Wcislik and S. Lipiec, Materials **15**, 6473 (2022).
[3] S. Curiotto, A. Chame, C. V. Thompson, P. Müller, and O. Pierre-Louis, Applied Physics Letters **120**, 091603 (2022).
[4] D. Yang, Y. C. Chan, and M. Pecht, *Electromigration in thin films and electronic devices: materials and reliability*, chapter Electromigration in flip-chip solder joints, page 285, Elsevier, 2011.
[5] S. Curiotto, P. Müller, A. El-Barraj, F. Cheynis, O. Pierre-Louis, F. Leroy, Applied Surface Science **469**, 463 (2019).
[6] L. K. Mansur, Journal of Nuclear Materials **216**, 97 (1994).
[7] C. C. Griffioen, J. H. Evans, P. C. De Jong, and A. Van Veen, Nuclear Instruments and Methods in Physics Research **B27**, 417 (1987).
[8] G. S. Was, Journal of Nuclear Materials **367-370**, 11 (2007).
[9] L. Gabrish, H. andKjeldgaard, E. Johnson, and U. Dahmen, Acta Materialia **49**, 4259 (2001). Radetic, T. and Johnson, E. and Olmsted, D.L. and Yang, Y. and Laird, B.B. and Asta, M. and Dahmen, U.
[10] T. Radetic, E. Johnson, D.L. Olmsted, Y. Yang, B.B. Laird, M. Asta, U. Dahmen Acta Materialia **141**, 427 (2017).
[11] F. A. Nichols, Journal of nuclear materials **30**, 143 (1969).
[12] L. E. Willertz and P. G. Shewmon, Metallurgical transactions **1**, 2217 (1970).
[13] P. J. Goodhew and S. K. Tyler, Proceedings of the Royal Society of London A **377**, 151 (1981).
[14] J. H. Evans, Nuclear Instruments and Methods in Physics Research **B196**, 125 (2002).
[15] K. D. Hammond, Materials Research Express **4**, 104002 (2017).
[16] G. R. Odette, M. J. Alinger, and B. D. Wirth, Annual Reviews of Materials Research **38**, 471 (2008).
[17] A. F. Voter, *Radiation Effects in Solids*, Springer, NATO Publishing Unit, Dordrecht, The Netherlands, 2005.
[18] for rough comparisons with real time, the attempt frequency could be taken equal to a typical atom vibration frequency, 10^{13} s^{-1}.
[19] L. Corso, S. Curiotto, E. Bernard, M. Cabie, C. Martin, L. Martinelli, F. Cheynis, P. Müller, F. Leroy, Nuclear Materials and Energy **37**, 101533 (2023).
[20] F. Silly and M. R. Castell, Applied Physics Letters **87**, 063106 (2005).
[21] B. Mutaftschiev, *The atomistic nature of Crystal Growth*, Springer series in materials science, 2001.
[22] Y. Saito, *Statistical Physics of Crystal Growth*, World Scientic, Singapore, 1996.
[23] R. Kern, G. Le Lay, and J.-J. Metois, *Basic mechanisms in the early stages of epitaxy*, North holland publishing Co, Current topics in materials science, Vol 3, editor E. Kaldis, 1979.

[24]O. Pierre-Louis, A. Chame, and Y. Saito, Physical Review Letters **99**, 136101 (2007).
[25]P. Ghosh and M. Ranganathan, Surface Science **630**, 174 (2014).
[26]J. Krug, H. T. Dobbs, and S. Majaniemi, Zeitschrift fur Physik B **97**, 281 (1995).
[27]N. Combe and H. Larralde, Physical review B **62**, 16074 (2000).
[28]D. A. Porter and E. K. E., *Phase transformations in metals and alloys*, Van Nostrand Reinhold Company Ltd., 1981.
[29]S. Curiotto, P. Müller, F. Cheynis, and F. Leroy, Applied Surface Science **552**, 149454 (2021).
[30]A. Bogicevic, S. Liu, J. Jacobsen, B. Lundqvist, and H. Metiu, Physical Review B **57**, R9459 (1998).
[31]S. Yashonath and P. Santikary, Journal of Physical Chemistry **98**, 6368 (1994).
[32]E. G. Derouane, J.-M. Andre, and A. A. Lucas, Journal of Catalysis **110**, 58 (1988).
[33]S. Yashonath and P. K. Ghorai, Journal of Physical Chemistry B **112**, 665 (2008).
[34]J. Yuan, M. Gao, Z. Liu, X. Tang, Y. Tian, G. Ma, M. Ye, A. Zheng, Nature Communications **14**, 1735 (2023).
[35]S. Nag, M. Sharma, and S. Yashonath, The Journal of Chemical Physics **153**, 244503 (2020).
[36]P. Wynblatt and N. A. Gjostein, Progress in Solid State Chemistry **9**, 21 (1975).
[37]F. Leroy, A. El-Barraj, F. Cheynis, P. Müller, and S. Curiotto, Physical Review Letters **123**, 176101 (2019).
[38]H. J. W. Zandvliet, O. Gurlu, and B. Poelsema, Physical Review B **64**, 073402 (2001).
[39]J. E. Avron, H. Van Beijeren, L. S. Schulman, and R. K. P. Zia, Journal of Physics A: Mathematical and General **15**, L81 (1982).
[40]R. Van Hardeveld and F. Hartog, Surface Science **15**, 189 (1969).
[41]F. H. Kaatz and A. Bultheel, Nano Express **14**, 150 (2019).
[42]K. C. Lai, D.-J. Liu, P. A. Thiel, and J. W. Evans, The Journal of Physical Chemistry C **122**, 11334 (2018).
[43]K. C. Lai, J. W. Evans, and D.-J. Liu, The Journal of Chemical Physics **147**, 201101 (2017).
[44]K. C. Lai, D.-J. Liu, and J. W. Evans, Physical Review B **96**, 235406 (2017).